Journal of Zhejiang University SCIENCE A
ISSN 1673-565X (Print); ISSN 1862-1775 (Online)
www.zju.edu.cn/jzus; www.springerlink.com
E-mail: jzus@zju.edu.cn

SOFC temperature evaluation based on an adaptive fuzzy controller

Xiao-juan WU†, Xin-jian ZHU, Guang-yi CAO, Heng-yong TU

(*Institute of Fuel Cell, Department of Automation, Shanghai Jiao Tong University, Shanghai 200030, China*)

†E-mail: xj_wu@sjtu.edu.cn

Received Oct. 28, 2007; revision accepted Dec. 25, 2007; published online Mar. 6, 2008

Abstract: The operating temperature of a solid oxide fuel cell (SOFC) stack is a very important parameter to be controlled, which impacts the performance of the SOFC due to thermal cycling. In this paper, an adaptive fuzzy control method based on an affine nonlinear temperature model is developed to control the temperature of the SOFC within a specified range. Fuzzy logic systems are used to approximate nonlinear functions in the SOFC system and an adaptive technique is employed to construct the controller. Compared with the traditional fuzzy and proportion-integral-derivative (PID) control, the simulation results show that the designed adaptive fuzzy control method performed much better. So it is feasible to build an adaptive fuzzy controller for temperature control of the SOFC.

Key words: Solid oxide fuel cell (SOFC), Temperature control, Adaptive fuzzy controller, Affine temperature model
doi:10.1631/jzus.A071569 **Document code:** A **CLC number:** TK01

INTRODUCTION

Solid oxide fuel cells (SOFCs) are energy conversion devices that produce electricity and heat directly by electrochemical reaction. For clean and efficient electrical power generation, the SOFC is a promising candidate for future energy conversion systems.

Performance of the SOFC stack is greatly related to its operating temperature. Due to its high operation temperature, the SOFC has many advantages, such as high energy conversion efficiency, flexibility of usable fuel type, and high temperature exhaust gas. However, too high temperatures may degrade the materials and too low temperatures impair power output. Consequently, the operating temperature of the SOFC stack must be controlled in a specified range with smaller fluctuations that ensure better performance of the SOFC.

For getting a better thermal management of the SOFC, it is necessary to develop a thermal model and find a suitable control method on the basis of this model. During the last several decades, various thermal models have been established in the research on the internal mechanisms of the SOFC (Larrain *et al*., 2003; Sanchez *et al*., 2006; Ivanov, 2007). However, these models have not given clear mathematical relations between the input gas velocities and the output temperature of SOFC. Reports about controlling the temperature of the SOFC stack are much less than those about the models. To our knowledge, only a few publications discussed the control problems of SOFC (Aguiar *et al*., 2005; Kaneko *et al*., 2006; Stiller *et al*., 2006). However, temperature control is only mentioned and the model-based control strategy is not discussed.

Consequently, an affine nonlinear temperature model of an SOFC stack is developed after analyzing the dynamic thermal transfer of Murshed *et al.*(2007) and Xi *et al.*(2007). Based on this temperature model, an adaptive fuzzy control method is presented to control the temperature of the SOFC in a specified range by regulating the gas velocities. The temperature model of the SOFC is a nonlinear system with disturbances and uncertainty. Therefore an adaptive controller with good control strategy is desirable for the SOFC stack. In recent years, based on the universal approximation theorem, several adaptive fuzzy control schemes have been developed for a class of nonlinear and uncertain systems (Chang, 2000; 2001;

Gazi and Passino, 2000). In this paper, fuzzy logic systems can be used to approximate nonlinear function in the SOFC system. Based on this observation, an adaptive technique is employed to construct the temperature controllers of the SOFC system.

DYNAMIC THERMAL MODEL OF SOFC

The proposed dynamic thermal model of a planar SOFC stack is based on the following assumptions: (1) All gases are ideal; (2) No temperature variation in the axial direction is observed; (3) The axial conduction heat transfer between nodes is neglected; (4) For the energy balance, pressure changes within the SOFC are negligible; (5) Adiabatic boundaries for the cell are required.

In this paper, there are mainly the following heat transfer processes in the SOFC stack: (a) the input heat energy of fuel gas; (b) heat convection between fuel gas and electrode; (c) heat convection between fuel gas and interconnect; (d) the fuel side heat generation due to mass transfer into the electrode porous space; (e) the input heat energy of air gas; (f) heat convection between air gas and electrode; (g) heat convection between air gas and interconnect; (h) the air side heat generation due to mass transfer into the electrode porous space; (i) ohmic heat produced by stack resistance; (j) heat radiation between electrode and interconnection of fuel side; (k) heat radiation between electrode and interconnection of air side.

Energy balance is performed around electrode, interconnector, fuel gas channel and air gas channel of the SOFC stack. Then the following relations can be obtained.

Energy balance around electrode

The electrode control volume consists of the anode, electrolyte and the cathode. Even though the electro-chemical reactions take place at the anode and cathode near the surfaces of the electrolyte, and thus have temperature variations in the direction vertical to the surface area, it can be assumed to be constant due to very small thickness of the electrode. The temperature variation along the flow direction is also assumed to be constant, and thus the electrode temperature T_e is affected by the heat transfer processes (b), (d), (f), (h), (i), (j) and (k). A heat balance is written as:

$$C_e \, \mathrm{d}T_e / \mathrm{d}t = Q_{fe} + Q_{ae} + Q_{rf} + Q_{ra} + Q_{react\_a} + Q_{react\_f} + Q_{ohimc}, \quad (1)$$

where $C_e=c_e\rho_e A w_e$, C_e is the heat capacity, and c_e, ρ_e, A, w_e are the specific heat, density, electro-chemical surface area and thickness of the electrode material, respectively.

The convective heat transfers between electrode and fuel/air gases can be written as:

$$Q_{fe} = k_{fe} A (T_f - T_e), \quad (2)$$

$$Q_{ae} = k_{ae} A (T_a - T_e). \quad (3)$$

Heat transfer coefficients k_{fe} and k_{ae} can be obtained as follows:

$$k = (Nu \times \lambda) / D, \quad (4)$$

where Nu is the Nusselt number, D and λ are the hydraulic diameters of the flow channel and the heat transfer coefficients, respectively.

The radiative heat transfer terms between electrode and interconnector of fuel side and air side in Eq.(1) can be expressed as:

$$Q_{rf} = \sigma A (T_i^4 - T_e^4) / ((1/\varepsilon_f) + (1/\varepsilon_i) - 1), \quad (5)$$

$$Q_{ra} = \sigma A (T_i^4 - T_e^4) / ((1/\varepsilon_a) + (1/\varepsilon_i) - 1), \quad (6)$$

where σ is the Boltzman constant; T_i is the interconnector temperature; ε_a, ε_f and ε_i are the emmisivity constants of cathode, anode and interconnector materials, respectively.

The air/fuel side heat generations due to mass transfer into the electrode porous space can be expressed as:

$$Q_{react\_a} = \frac{I}{4F} h_{O_2}, \quad (7)$$

$$Q_{react\_f} = \frac{I}{2F} (h_{H_2} - h_{H_2O}), \quad (8)$$

where I is the current density and F is Faraday constant; h_{O_2}, h_{H_2} and h_{H_2O} are heat generation of 1 mol O_2, H_2 and H_2O, respectively.

The ohmic heat generation produced by stack resistance can be expressed as:

$$Q_{\text{ohimc}} = IV. \tag{9}$$

Energy balance around interconnector

The interconnector temperature T_i is affected by the heat transfer processes (c), (g), (j) and (k). A heat balance is written as:

$$C_i \mathrm{d}T_i / \mathrm{d}t = Q_{\text{fi}} + Q_{\text{ai}} - Q_{\text{rf}} - Q_{\text{ra}}, \tag{10}$$

where $C_i=c_i\rho_i A w_i$, C_i is the heat capacity, and c_i, ρ_i and w_i are the specific heat, density and thickness of the interconnector material, respectively.

Convective heat transfers between interconnect and fuel/air can be expressed as:

$$Q_{\text{fi}} = k_{\text{fi}} A(T_f - T_i), \tag{11}$$

$$Q_{\text{ai}} = k_{\text{ai}} A(T_a - T_i), \tag{12}$$

where k_{fi} and k_{ai} are heat transfer coefficients.

Energy balance around fuel side

The dynamic model of exit fuel temperature T_f is affected by the heat transfer processes (a), (b), (c) and (d). A heat balance is written as:

$$C_f \,\mathrm{d}T_f / \mathrm{d}t = Q_f^{\text{in}} - Q_{\text{fi}} - Q_{\text{fe}} - Q_{\text{react\_f}}, \tag{13}$$

where $C_f=c_f\rho_f s_f w_f$, C_f is the heat capacity, c_f, ρ_f, s_f and w_f is the specific heat, density, cross-sectional area and height of the fuel gas channel material, respectively.

The inlet enthalpy flux, Q_f^{in} depends on the fuel inlet conditions:

$$Q_f^{\text{in}} = q_f (T_{\text{in\_f}} - T_f), \tag{14}$$

$$q_f = c_{\text{in\_f}} \rho_{\text{in\_f}} s_f v_f, \tag{15}$$

where v_f is the fuel velocity.

Energy balance around air side

The dynamic model of air exit temperature T_a is affected by the heat transfer processes (e), (f), (g) and (h). A heat balance is written as:

$$C_a \,\mathrm{d}T_a / \mathrm{d}t = Q_a^{\text{in}} - Q_{\text{ae}} - Q_{\text{ai}} - Q_{\text{react\_a}}, \tag{16}$$

where $C_a=c_a\rho_a s_a w_a$, C_a is the heat capacity, c_a, ρ_a, s_a, w_a are the specific heat, density, cross-sectional area and height of the air gas channel material, respectively.

The inlet enthalpy flux, Q_a^{in} is dependent upon the air inlet conditions:

$$Q_a^{\text{in}} = q_a (T_{\text{in\_a}} - T_a), \tag{17}$$

$$q_a = c_{\text{in\_a}} \rho_{\text{in\_a}} s_a v_a, \tag{18}$$

where v_a is the air velocity.

A number of additional quantities are defined:

$$
\begin{aligned}
& a_1 = k_{\text{fe}} A / C_e, \;\; a_2 = k_{\text{ae}} A / C_e, \\
& a_3 = \sigma A / \{[(1/\varepsilon_f) + (1/\varepsilon_i) - 1] C_e\} \\
& \qquad + \sigma A / \{[(1/\varepsilon_a) + (1/\varepsilon_i) - 1] C_e\}, \\
& a_4 = I, \\
& a_5 = V / C_e + h_{O_2} / (4FC_e) + (h_{H_2} - h_{H_2O}) / (2FC_e), \\
& a_6 = k_{\text{fi}} A / C_i, \;\; a_7 = k_{\text{ai}} A / C_i, \\
& a_8 = \sigma A / \{[(1/\varepsilon_f) + (1/\varepsilon_i) - 1] C_i\} \\
& \qquad + \sigma A / \{[(1/\varepsilon_a) + (1/\varepsilon_i) - 1] C_i\}, \\
& b_1 = c_{\text{in\_f}} \rho_{\text{in\_f}} s_f / C_f, \;\; u_1 = v_f, \\
& a_9 = k_{\text{fe}} A / C_f, \;\; a_{10} = k_{\text{fi}} A / C_f, \\
& a_{11} = (h_{H_2} - h_{H_2O}) / (2FC_f), \\
& b_2 = c_{\text{in\_a}} \rho_{\text{in\_a}} s_a / C_a, \\
& u_2 = v_a, \; a_{12} = k_{\text{ae}} A / C_a, \;\; a_{13} = k_{\text{ai}} A / C_a, \\
& a_{14} = h_{O_2} / (4FC_a),
\end{aligned}
$$

The state variable is

$$\boldsymbol{x} = [x_1, x_2, x_3, x_4]^{\mathrm{T}} = [T_e, T_i, T_f, T_a]^{\mathrm{T}}.$$

The manipulated variable is

$$\boldsymbol{u} = [v_f, v_a]^{\mathrm{T}}.$$

The controlled variable is

$$\boldsymbol{y} = [y_1, y_2, y_3, y_4]^{\mathrm{T}} = [x_1, x_2, x_3, x_4]^{\mathrm{T}}.$$

Using the above definitions, the temperature model of the SOFC stack can be described by Eq.(19), which is a normative affine form:

$$\begin{cases} \dot{\boldsymbol{x}}=f(\boldsymbol{x})+g(\boldsymbol{x})\boldsymbol{u}, \\ \boldsymbol{y}=\boldsymbol{x}, \end{cases} \tag{19}$$

where

$$f(\boldsymbol{x})=\begin{bmatrix} a_1(x_3-x_1)+a_2(x_4-x_1)+a_3(x_2^4-x_1^4)+a_4a_5 \\ a_6(x_3-x_2)+a_7(x_4-x_2)-a_8(x_2^4-x_1^4) \\ a_9(x_1-x_3)+a_{10}(x_2-x_3)-a_4a_{11} \\ a_{12}(x_1-x_4)+a_{13}(x_2-x_4)-a_4a_{14} \end{bmatrix},$$

$$g(x)=\begin{bmatrix} 0 & 0 \\ 0 & 0 \\ b_1(x_{30}-x_3) & 0 \\ 0 & b_2(x_{40}-x_4) \end{bmatrix}.$$

The main operating parameters of the SOFC stack are given in Table 1.

Table 1 Material properties of cell components

Parameter	Value	Reference
w_e (mm)	0.25	Murshed *et al*.(2007)
w_i (mm)	1.5	Murshed *et al*.(2007)
ρ_a (g/cm³)	5.8×10^{-4}	Damm and Fedorov (2006)
ρ_e (g/cm³)	6.6	Murshed *et al*.(2007)
ρ_f (g/cm³)	2×10^{-4}	Damm and Fedorov (2006)
ρ_i (g/cm³)	6.11	Murshed *et al*.(2007)
c_e, c_i (J/(g·K))	0.4	Murshed *et al*.(2007)
c_a (J/(g·K))	1.051	Damm and Fedorov (2006)
c_f (J/(g·K))	5	Damm and Fedorov (2006)
Nu	4	Stiller *et al*.(2005)
D_f (mm)	0.7	Stiller *et al*.(2005)
D_a (mm)	1.953	Stiller *et al*.(2005)
A (cm²)	100	Murshed *et al*.(2007)
λ_f (W/(m·K))	0.43	Lin and Beale (2003)
λ_a (W/(m·K))	0.075	Lin and Beale (2003)
σ (W/(m²·K⁴))	5.6704×10^{-8}	Murshed *et al*.(2007)
ε_a, ε_f, ε_i	0.9	Murshed *et al*.(2007)
w_f, w_a (mm)	1	Lin and Beale (2003)
ε_f, ε_a, ε_i	0.9	Murshed *et al*.(2007)

ADAPTIVE FUZZY CONTROLLER FOR SOFC

Fuzzy system

Center-average defuzzifier, product inference, and singleton fuzzifier are used. The output of the fuzzy system can be formulated as:

$$\hat{f}(\boldsymbol{x}|\boldsymbol{\theta}_f)=\sum_{j=1}^{m} y^j\left(\prod_{i=1}^{n}\mu_{A_i^j}(x_i)\right)\Big/\sum_{j=1}^{m}\left(\prod_{i=1}^{n}\mu_{A_i^j}(x_i)\right), \tag{20}$$

where $\mu_{A_i^j}$ is the membership function of x_i. If we fix the $\mu_{A_i^j}$ and view the y^j as adjustable parameters, then Eq.(20) can be written as:

$$\hat{f}(\boldsymbol{x}|\boldsymbol{\theta}_f)=\boldsymbol{\theta}_f^{\mathrm{T}}\boldsymbol{\zeta}(\boldsymbol{x}), \tag{21}$$

where $\boldsymbol{\theta}_f=[y^1,\cdots,y^m]^{\mathrm{T}}$ is the parameter vector of the fuzzy system $\hat{f}$, and $\boldsymbol{\zeta}(\boldsymbol{x})=[\zeta^1(x),\cdots,\zeta^m(x)]^{\mathrm{T}}$ is the vector of fuzzy basis functions defined as

$$\boldsymbol{\zeta}(\boldsymbol{x})=\prod_{i=1}^{n}\mu_{A_i^j}(x_i)\Big/\sum_{j=1}^{m}\left(\prod_{i=1}^{n}\mu_{A_i^j}(x_i)\right). \tag{22}$$

Similarly we can get the fuzzy identification system $\hat{g}(\boldsymbol{x}|\boldsymbol{\theta}_g)$ of the form Eq.(23) for approximating $g(\boldsymbol{x})$

$$\hat{g}(\boldsymbol{x}|\boldsymbol{\theta}_g)=\boldsymbol{\theta}_g^{\mathrm{T}}\boldsymbol{\eta}(\boldsymbol{x}), \tag{23}$$

where $\boldsymbol{\theta}_g$ is the parameter vector of the fuzzy system $\hat{g}$, and $\boldsymbol{\eta}(\boldsymbol{x})$ is the vector of fuzzy basis functions.

Controller

Now consider the problem of controlling the system Eq.(19). If the plant is known, the functions $f(\boldsymbol{x})$ and $g(\boldsymbol{x})$ are used to construct the following feedback control law (Slotine and Li, 1991):

$$u^*=(1/g(\boldsymbol{x}))[-f(\boldsymbol{x})+y_m^{(n)}+\boldsymbol{K}^{\mathrm{T}}\boldsymbol{e}], \tag{24}$$

where $\boldsymbol{e}=\boldsymbol{y}_m-\boldsymbol{y}=\boldsymbol{y}_m-\boldsymbol{x}$ is the tracking error, $\boldsymbol{e}=(e,\dot{e},\ldots,e^{(n-1)})^{\mathrm{T}}$ and $\boldsymbol{K}=(k_n,\ldots,k_1)^{\mathrm{T}}$ are chosen such that all roots of the polynomial $h(s)=s^n+k_1s^{(n-1)}+\cdots+k_n$ are in the open left-half of the complex plane.

However, since f and g are unknown, we cannot use them for constructing the control law Eq.(24). Therefore, in the following, we replace them by their estimates $\hat{f}$ and $\hat{g}$ to construct a self-tuning controller

$$u^* = 1/\hat{g}(\boldsymbol{x}|\boldsymbol{\theta}_g)[-\hat{f}(\boldsymbol{x}|\boldsymbol{\theta}_f) + y_m^{(n)} + \boldsymbol{K}^{\mathrm{T}}\boldsymbol{e}], \quad (25)$$

where $\boldsymbol{\theta}_f$ and $\boldsymbol{\theta}_g$ are the parameters of the approximating systems $\hat{f}$ and $\hat{g}$, respectively. Applying the control law Eq.(25) to the system Eq.(19), after some manipulation, results in the error dynamic equation

$$\dot{\boldsymbol{e}} = \boldsymbol{\Lambda e} + \boldsymbol{b}\{[\hat{f}(\boldsymbol{x}|\boldsymbol{\theta}_f) - f(\boldsymbol{x})] + [\hat{g}(\boldsymbol{x}|\boldsymbol{\theta}_g) - g(\boldsymbol{x})]\boldsymbol{u}\}, \quad (26)$$

where

$$\boldsymbol{\Lambda} = \begin{bmatrix} 0 & 1 & 0 & 0 \\ \vdots & \vdots & \vdots & \vdots \\ 0 & 0 & 0 & 1 \\ -k_n & -k_{n-1} & \cdots & -k_1 \end{bmatrix}, \quad \boldsymbol{b} = \begin{bmatrix} 0 \\ 0 \\ \vdots \\ 0 \\ 0 \end{bmatrix}.$$

Now, consider the following optimal parameter vectors:

$$\boldsymbol{\theta}_f^* = \arg\min_{\boldsymbol{\theta}_f \in \boldsymbol{\Omega}_f} \left[\sup_{x\in\mathbb{R}^n} \left| \hat{f}(\boldsymbol{x}|\boldsymbol{\theta}_f) - f(\boldsymbol{x}) \right| \right], \quad (27)$$

$$\boldsymbol{\theta}_g^* = \arg\min_{\boldsymbol{\theta}_g \in \boldsymbol{\Omega}_g} \left[\sup_{x\in\mathbb{R}^n} \left| \hat{g}(\boldsymbol{x}|\boldsymbol{\theta}_g) - g(\boldsymbol{x}) \right| \right]. \quad (28)$$

By defining the minimum approximation error:

$$\boldsymbol{w} = [\hat{f}(\boldsymbol{x}|\boldsymbol{\theta}_f^*) - f(\boldsymbol{x})] + [\hat{g}(\boldsymbol{x}|\boldsymbol{\theta}_f^*) - g(\boldsymbol{x})]\boldsymbol{u}, \quad (29)$$

the error Eq.(26) can be written as follows:

$$\dot{\boldsymbol{e}} = \boldsymbol{\Lambda e} + \boldsymbol{bw} + \boldsymbol{b}\{[\hat{f}(\boldsymbol{x}|\boldsymbol{\theta}_f) - \hat{f}(\boldsymbol{x}|\boldsymbol{\theta}_f^*)] + [\hat{g}(\boldsymbol{x}|\boldsymbol{\theta}_g) - \hat{g}(\boldsymbol{x}|\boldsymbol{\theta}_g^*)]\boldsymbol{u}\}. \quad (30)$$

By substituting Eqs.(21) and (23) in Eq.(30), we have:

$$\dot{\boldsymbol{e}} = \boldsymbol{\Lambda e} + \boldsymbol{bw} + \boldsymbol{b}\{[(\boldsymbol{\theta}_f - \boldsymbol{\theta}_f^*)^{\mathrm{T}}\boldsymbol{\zeta}(\boldsymbol{x})] + [(\boldsymbol{\theta}_g - \boldsymbol{\theta}_g^*)^{\mathrm{T}}\boldsymbol{\eta}(\boldsymbol{x})]\boldsymbol{u}\}. \quad (31)$$

Adaptive law

In this section, we develop an adaptive algorithm for adjusting the parameters of the self-tuning fuzzy controller Eq.(26). The goal of parameter adjustment is to make $\boldsymbol{\theta}_f \to \boldsymbol{\theta}_f^*$ and $\boldsymbol{\theta}_g \to \boldsymbol{\theta}_g^*$, and consequently, make $(\hat{f}(\boldsymbol{x}|\boldsymbol{\theta}_f), \hat{g}(\boldsymbol{x}|\boldsymbol{\theta}_g))$ a good estimate of $(f(\boldsymbol{x}), g(\boldsymbol{x}))$.

Now we consider the following Lyapunov function candidate (Sastry and Bodson, 1989):

$$V = \boldsymbol{e}^{\mathrm{T}}\boldsymbol{Pe}/2 + (\boldsymbol{\theta}_f - \boldsymbol{\theta}_f^*)^{\mathrm{T}}(\boldsymbol{\theta}_f - \boldsymbol{\theta}_f^*)/(2r_1) + (\boldsymbol{\theta}_g - \boldsymbol{\theta}_g^*)^{\mathrm{T}}(\boldsymbol{\theta}_g - \boldsymbol{\theta}_g^*)/(2r_2), \quad (32)$$

where r_1 and r_1 are positive constants. $\boldsymbol{P}$ is an unique positive-definite symmetric matrix which satisfies the Lyapunov equation below:

$$\boldsymbol{\Lambda}^{\mathrm{T}}\boldsymbol{P} + \boldsymbol{P\Lambda} = -\boldsymbol{Q}, \quad (33)$$

where $\boldsymbol{Q}$ is an arbitrary positive-definite symmetric matrix. The time derivative of V along the trajectories of Eq.(31) equals:

$$\left.\frac{\mathrm{d}V}{\mathrm{d}t}\right|_{(31)} = -\boldsymbol{e}^{\mathrm{T}}\boldsymbol{Qe}/2 + \boldsymbol{e}^{\mathrm{T}}\boldsymbol{Pbw} + (\boldsymbol{\theta}_f - \boldsymbol{\theta}_f^*)^{\mathrm{T}}/r_1 \times[\dot{\boldsymbol{\theta}}_f + r_1\boldsymbol{e}^{\mathrm{T}}\boldsymbol{Pb\zeta}(\boldsymbol{x})] + (\boldsymbol{\theta}_g - \boldsymbol{\theta}_g^*)^{\mathrm{T}}/r_2 \times[\dot{\boldsymbol{\theta}}_g + r_2\boldsymbol{e}^{\mathrm{T}}\boldsymbol{Pb\eta}(\boldsymbol{x})\boldsymbol{u}]. \quad (34)$$

Based on Eq.(34), Wang (1994) has proposed the following adaptive law for adjusting the parameters:

$$\dot{\boldsymbol{\theta}}_f = -r_1\boldsymbol{e}^{\mathrm{T}}\boldsymbol{Pb\zeta}(\boldsymbol{x}), \quad (35)$$

$$\dot{\boldsymbol{\theta}}_g = -r_2\boldsymbol{e}^{\mathrm{T}}\boldsymbol{Pb\eta}(\boldsymbol{x}). \quad (36)$$

SIMULATION AND DISCUSSION

The SOFC stack has two inputs and four outputs. Because the temperature responses of electrode, interconnector, fuel and air side of the SOFC stack are somewhat similar, and for the space limitation, we only give the simulation results of the electrode temperature of the SOFC stack in this paper. Under various gas velocities, the electrode temperature response is shown in Fig.1.

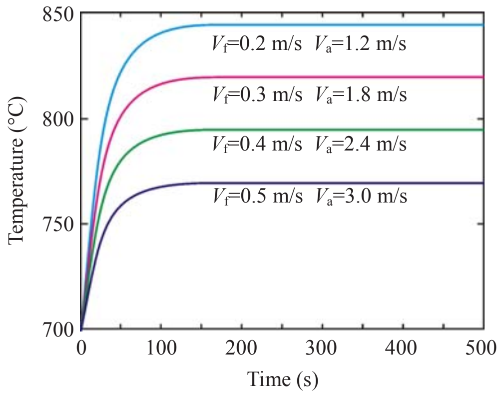

Fig.1 Electrode temperature under various gas velocities

Now we use the proposed adaptive fuzzy controller to control the temperature of the SOFC stack. Firstly we control the temperature to track the stable temperature 800 °C. The initial temperatures are all assumed 700 °C. Define three fuzzy sets over each aixs. Therefore, the number of fuzzy rules used to approximate $f(\boldsymbol{x})$ and $g(\boldsymbol{x})$ is 81. We choose k_1=5, k_2=9, k_3=7 and k_4=2 (so that $s^4+k_1s^3+k_2s^2+k_3s+k_4$ is stable), and $\boldsymbol{Q}$=diag(5,5,5,5). The initial $\boldsymbol{\theta}_f(0)$ and $\boldsymbol{\theta}_g(0)$ are chosen randomly in the intervals [−4, 4]. The simulation result is shown in Fig.2. From Fig.2, we can see that the proportion-integral-derivative (PID) controller is incapable of controlling the operating temperature to the target value. The result of traditional fuzzy control is similar to that of the adaptive fuzzy control. However, if the control processes go beyond the coverage of the initial rules, the performance of traditional fuzzy control deteriorates greatly.

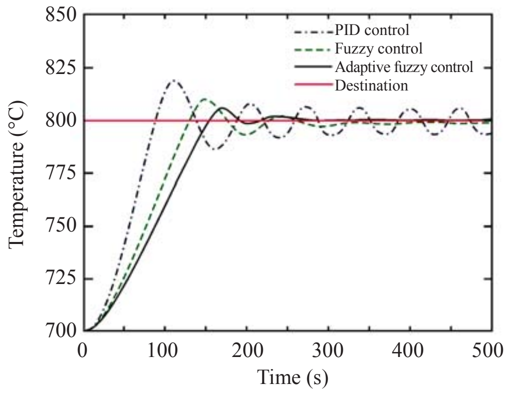

Fig.2 Experimental results with three control methods

Assuming that the external load of the SOFC stack has a 20% step change from initial stack temperature 780 °C, the simulation result is shown in Fig.3. From Fig.3, we can get the following conclusions: the adaptive fuzzy controller can regulate and control the stack temperature to change smoothly to destination stabilization value, more quickly and with smaller undulation than the PID and traditional fuzzy control without cluster analysis.

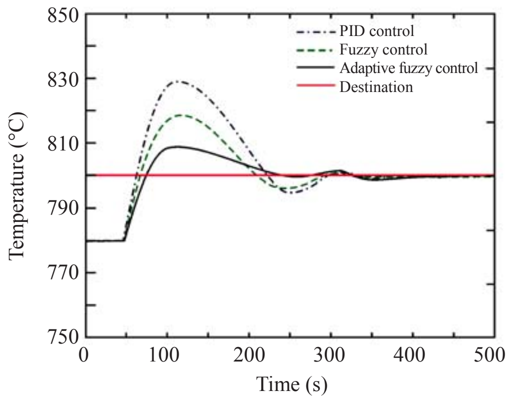

Fig.3 Experimental results of the SOFC temperature at initial temperature 780 °C

CONCLUSION

The operating temperature of the stack is the most important variable in the SOFC system. In order to better control the temperature, an affine nonlinear temperature model of the SOFC stack is developed based on the energy conservation. Since the model is a nonlinear model with uncertain parameters and disturbance, an adaptive fuzzy controller is designed for the SOFC system. Numerical experimental results show the validity of the proposed controller.

References

Aguiar, P., Adjiman, C., Brandon, N., 2005. Anode-supported intermediate temperature direct internal reforming solid oxide fuel cell. II. Model-based dynamic performance and control. *Journal of Power Sources*, **147**(1-2):136-147. [doi:10.1016/j.jpowsour.2005.01.017]

Chang, Y.C., 2000. Robust tracking control for nonlinear MIMO systems via fuzzy approaches. Automatica, **36**(10):1535-1545. [doi:10.1016/S0005-1098(00)00083-2]

Chang, Y.C., 2001. Adaptive fuzzy-based tracking control for nonlinear SISO systems via VSS and H_∞ approaches. *IEEE Transaction on Fuzzy Systems*, **9**(2):278-292. [doi:10.1109/91.919249]

Damm, D.L., Fedorov, A.G., 2006. Reduced-order transient thermal modeling for SOFC heating and cooling. *Journal of Power Sources*, **159**(2):956-967. [doi:10.1016/ j.jpowsour.2005.11.072]

Gazi, V., Passino, K.M., 2000. Direct Adaptive Control Using Dynamic Structure Fuzzy Systems. Proceeding of the American Control Conference. Chicago, IL, p.1954-1958.

Ivanov, P., 2007. Thermodynamic modeling of the power plant based on the SOFC with internal steam reforming of methane. *Electrochimica Acta*, **52**(12):3921-3928. [doi:10.1016/j.electacta.2006.11.009]

Kaneko, T., Brouwer, J., Samuelsen, G.S., 2006. Power and temperature control of fluctuating biomass gas fueled solid oxide fuel cell and micro gas turbine hybrid system. *Journal of Power Sources*, **160**(1):316-325. [doi:10.1016/j.jpowsour.2006.01.044]

Larrain, D., van Herle, J., Marechal, F., Favrat, D., 2003. Thermal modeling of a small anode supported solid oxide fuel cell. *Journal of Power Sources*, **118**(1-2):367-374. [doi:10.1016/S0378-7753(03)00102-2]

Lin, Y., Beale, S.B ,2003. Numerical Simulations of the Performance of a Planar Solid-oxide Fuel Cell Stack. Proceedings CFD 2003, 11th Annual Conference of the CFD Society of Canada, Vancouver.

Murshed, A.M., Huang, B., Nandakumar, K., 2007. Control relevant modeling of planer solid oxide fuel cell system. *Journal of Power Sources*, **163**(2):830-845. [doi:10.1016/ j.jpowsour.2006.09.080]

Sanchez, D., Chacartegui, R., Munoz, A., Sanchez, T., 2006. Thermal and electrochemical model of internal reforming oxide fuel cells with tubular geometry. *Journal of Power Sources*, **160**(2):1074-1087. [doi:10.1016/j.jpowsour.2006.02.098]

Sastry, S., Bodson, M., 1989. Adaptive Control: Stability, Convergence and Robustness. Upper Saddle River, Prentice-Hall, NJ.

Slotine, J.J, Li, W., 1991. Applied Nonlinear Control. Englewood Cliffs, Prentice-Hall, NJ.

Stiller, C., Thorud, B., Seljebø, S., Mathisen, Ø., Karoliussen, H., Bolland, O., 2005. Finite-volume modeling and hybrid-cycle performance of planar and tubular solid oxide fuel cells. Journal of Power Sources, **141**(2):227-240. [doi:10.1016/j.jpowsour. 2004. 09.019]

Stiller, C., Thorud, B., Bolland, O., Kandepu, R., Imsland, L., 2006. Control strategy for a solid oxide fuel cell and gas turbine hybrid system. *Journal of Power Sources*, **158**(1):303-315. [doi:10.1016/j.jpowsour.2005.09.010]

Wang, L.X., 1994. Adaptive Fuzzy Systems and Control: Design and Stability Analysis. Upper Saddle River, Prentice-Hall, NJ.

Xi, H., Sun. J., Tsourapas, V., 2007. A control oriented low order dynamic model for planar SOFC using minimum Gibbs free energy method. *Journal of Power Sources*, **165**(1):253-266. [doi:10.1016/j.jpowsour.2006.12.009]